

4.13 Report of Project Part 13: Mesoscopic theory of quantum devices

Theory of optical properties and carrier transport of mid-infrared quantum-dot devices

Principal investigator: **Peter Vogl**

Technische Universität München

Walter Schottky Institut

Am Coulombwall 3, 85748 Garching, Germany

Phone: +49 89 289 12750

Fax: +49 89 289 12737

eMail: vogl@wsi.tum.de

4.13.1 Summary

The main goal of this project has been to study, optimize, and design novel device geometries of THz quantum cascade laser structures in a broad range of materials and material geometries, involving quantum wells, quantum wires, and quantum dots. From a theory point of view, the method of choice for quantitative predictions for carrier dynamics in open, dissipative quantum systems is the Keldysh or non-equilibrium Green's function technique (NEGF), and our aim was to push this method forward to render realistic predictions of complex nanostructures such as quantum cascade lasers possible. Since realistic calculations of nanodevices require not only an intimate treatment of carrier dynamics but also of the electronic structure, we devoted a significant portion of our research on extending our mesoscopic envelope-type function scheme nextnano to be able to cover doped or undoped structures, biased or unbiased materials, finite or broken gap semiconductors or semimetals, all within the same consistent theoretical scheme.

We have published these collaborative efforts in 33 refereed journal papers so far and presented our results in numerous international conferences with a total of 7 invited papers. Up to now, only 3 of the published papers have been coauthored with the experimental groups within the IR-ON (Deutsch 2010, Kubis 2009d, Brehm 2008). Actually, however, we have been and still are intensely collaborating with the experimental groups but experiments simply take significantly longer than theoretical predictions. Therefore, all of us anticipate a fair amount of additional publications once more of the experiments that we have proposed have actually been performed.

One of our principal results is the prediction of room temperature operation for quantum cascade lasers (QCL) in the THz regime that are based on III-V nanowire heterostructures as we will detail below. In addition, we predict novel designs of quantum well QCL that promise a significant increase in gain relative to present day standard designs (Kubis 2008, Kubis 2009/a-c, Yasuda 2009). Our calculations have also provided essential guidance for the novel Type II InGaAs/GaAsSb/InP QCL developed by the Vienna group within this collaboration (Deutsch 2010).

Theory-wise, we have been able to clarify and assess the validity, applicability, commonly used approximations, as well as classical and quantum limits, of the NEGF method (Kubis 2011, Vogl 2010, Greck 2010). These results will help other researchers to implement this method with more confidence and deeper insight.

4.13.2 Scientific Background - State of the Art

The development of efficient THz QCLs relies on the control of both their electronic structure and their electronic transport properties. A theoretical investigation of the charge carrier dynamics in these devices is particularly challenging since it involves, at the same time, pronounced quantum mechanical effects as well as dissipation due to numerous interactions of the carriers with the environment. So far different methods for simulating QCLs have been reported in the literature: semi-classical Monte Carlo (Jirauschek 2007), density matrix (Savic 2007), and the non-equilibrium Green's function (NEGF) formalism (Wacker 2002, Lake 1997, Lee 2002, Vukmirovic 2007). Severe limitations are inherent to the first two mentioned methods. Semi-classical simulations are unable to catch the important effect of resonant tunneling, while density matrix approaches generally fail in predicting the gain spectra of THz QCLs, given the relatively large broadening of the optical transitions. The NEGF formalism, on the other hand, provides a general framework that allows one to faithfully incorporate all the important physical effects that come into play in these devices.

The NEGF theory has been developed almost 50 years ago by Keldysh and, independently, by Kadanoff and Baym, but a quantitative implementation of this formalism in semiconductor heterostructures is still a highly challenging task that only a few groups have carried out so far (Wacker 2002, Lee 2002, Lake 1997, Vukmirovic 2007, Schmielau 2009, Kubis 2009d). The complexity and at the same time power of NEGF-based simulation compared to previously mentioned methods lies in the fact that all relevant observables quantities such as local state populations, resonances, energy resolved density of states, etc. are resolved. In addition, when dissipation is considered, a self-consistent resolution scheme is needed, which renders the method highly time consuming.

At the beginning of the project, we had to face and address a number of issues that had to be resolved as a prerequisite for developing an efficient and accurate simulation scheme for the large variety of QCL devices that we intended to study.

1. An efficient implementation of the NEGF method to QCLs calls for approximations that have not been assessed in previous studies. In particular, all previous studies have assumed a priori that the charge distribution strictly follows the periodicity of the active zones. Nonperiodic effects, such as coherent tunnelling through extended states across one or several QCL periods, hot electron effects, or differences near source and drain contacts are left out by such methods.
2. A design optimization of QCLs requires the variation of many materials and device geometry parameters and therefore calls for methods that may be less accurate than a full NEGF implementation, but allow one to scan a large phase space quickly to identify the most promising materials combination, layer thicknesses and doping concentrations. Standard

NEGF implementations for QCLs do not fulfill this condition and require computer times exceeding one week for a single I-V characteristics.

3. Despite efforts in THz QCL design optimization, room temperature operation seems to be out of reach with planar quantum well material systems. One way to bypass this limitation is to use novel systems with reduced dimensionality such as nanowires or quantum dots. However, no theoretical tools have been developed so far that realistically predict electronic transport and optical gain in such systems. Simple model calculations of quantum wire based QCLs, however, have shown highly promising results (Wingreen 1997, Dmitriev 2005, Vukmirovic 2008).

4. Antimonide materials have a number of properties that makes them favourable candidates for mid-infrared lasers: the gap is widely tunable, the split-off band lies far away from the band gap which reduces Auger processes, and laser transitions across the energy gap reduce the efficiency of phonon emission due to the opposite dispersion of conduction and valence bands as opposed to subband emission (see e.g., Poulter 1999, Xu 2008). Unfortunately, the standard effective mass theory fails for materials with broken gaps since this method depends on an unambiguous separation into electron and hole states. Consequently, only a few theoretical approaches have been developed so far (Semenikhin 2007, Xu 2007) to predict the electronic structure of mesoscopic nanostructures with broken gaps.

We have addressed all of those aspects and issues and developed methods that have generated a fair number of interesting and promising predictions that will be presented in the subsequent section.

4.13.3 Results and Discussion

Rather than discussing all of our results, we will focus on three primary results that we obtained in the last funding period of this collaborative program.

Theory of nanowire quantum cascade lasers

We have investigated theoretically a new type of quantum cascade laser (QCL) made of embedded nanowire heterostructures instead of planar quantum wells. We have performed realistic calculations of the electrical and optical properties of these devices in terms of the non-equilibrium Green's function approach (NEGF). For narrow nanowires, our calculations predict a strong reduction of the current threshold and an increase of the maximum laser operation temperature up to room temperature in the THz region.

Quantum cascade lasers usually consist of planar quantum wells heterostructures. Their performances in terms of output power and operating temperature, especially for optical transition frequencies in the terahertz (THz) range, are still limited in spite of many efforts of

optimization in the past few years. At elevated temperature, non-radiative scattering processes assisted by phonon emission/absorption are enhanced, and THz lasing is prevented by (i) a poor population inversion and (ii) a strong broadening of the optical transition.

We propose the use of (core-shell) nanowires with axial superlattice heterostructure instead of planar quantum well heterostructure. The underlying idea is to take advantage of a reduction of dimensionality to inhibit the non-radiative relaxation mechanisms, as evidenced for THz intersublevel transitions in 0-D-like quantum dots (QDs) systems (Zibik 2009). To investigate the possible improvement of the QCLs properties with the lateral confinement, we have developed a model that includes the two limiting cases of coupled 0-D quantum dots and coupled 2-D planar quantum wells.

We have calculated the transport in a nanowire superlattice heterostructure in the non-equilibrium Green functions (NEGF) framework (Kubis 2009d), in which the various scattering mechanisms are treated within the self-consistent Born approximation (SCBA). Contrarily to previous approaches for planar QCLs that use 1-D real space (Lake 1997) or a Wannier basis (Wacker 2002), we have implemented a 3-D mode-space approach with a Wannier-Stark basis in the growth direction and field-periodic boundary conditions.

We have incorporated the scattering mechanisms due to interaction with optical and acoustic phonons, as well as interface and surface roughness scattering. In addition, an important scattering mechanism in quasi zero-dimensional systems is provided by the anharmonic decay of polarons (Grange 2007, Zibik 2009). For small nanowire diameters, we find that the strong coupling regime between electron and optical phonons leading to polaron formation is well described within the SCBA, in agreement with previous studies (Vukmirovic 2007). In order to treat the polaron anharmonicity (Grange 2007), we have implemented interacting LO-phonon Green functions whose self-energies include cubic anharmonic couplings to the two-phonon reservoir.

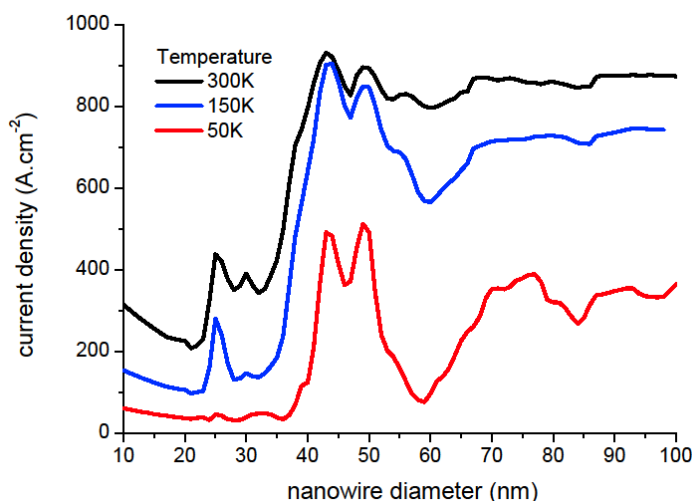


Figure 1: Current density in a nanowire-based InGaAs/GaAsSb QCL as a function of the nanowire diameter for various temperatures. The applied voltage bias is fixed to 50 mV per QCL period

An InGaAs/GaAsSb superlattice with three wells per QCL period, similar to the one studied by the Vienna optics group (Deutsch 2010), is considered. The calculated current density is presented in Fig. 1 as a function of the nanowire diameter for various temperatures. By varying the diameter, we observe a transition from the limit of coupled 0-D-like QDs (diameters below 30 nm) to the one of coupled 2-D quantum wells, associated with a large increase in the current density. In between, current peaks are found to correspond to resonances between the axial and lateral transition energies. In particular, the current peak for diameters around 45 nm is associated with the resonance between the lasing transition energy and the ground to first lateral excited state. When this resonance occurs, the electrons can scatter elastically from the upper laser state to the lower one by transferring the associated energy into a lateral motion. This transition of dimensionality from coupled 0-D to coupled 2-D wells is also clearly observed in the energy resolved electron density (not shown here).

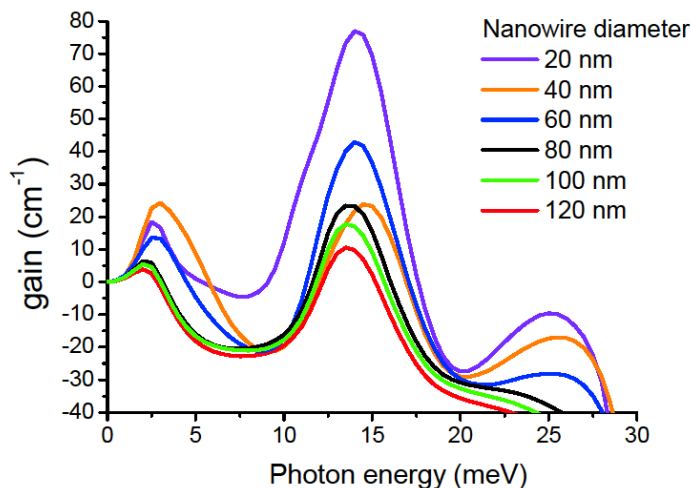


Figure 2: Optical gain in a nanowire-based InGaAs/ GaAsSb QCL at 300K as a function of photon energy for various nanowire diameters

The calculated optical gain at room temperature is reported on Fig. 2 for various diameters ranging from 20 to 120 nm. A dramatic increase of the THz gain is observed when reducing the nanowire diameter. This increase is non-monotonous: for diameters around the resonance mentioned above, a quenching of the gain is observed due to the efficient elastic scattering, as seen for a diameter of 40 nm on Fig. 2. For a diameter of 60 nm, the gain at room temperature reaches 40 cm⁻¹, which is higher than the material expected losses.

Novel, highly efficient quantum transport theory based on the non equilibrium Green's function method

A full implementation of the non-equilibrium Green's function method even for stationary transport problems in open quantum systems requires the self-consistent solution of two Green's functions. The first Green's function G^R characterizes the width and energy of the scattering states, whereas the second one $G^<$ characterizes the state occupancy and

determines the charge and current density. Each of these functions depends on 5 variables even for multi-quantum well structures that are laterally homogeneous (2 spatial coordinates, 2-dimensional momentum, and energy). The self-consistent solution cycle involves the solution of 4 coupled integro-differential equations.

While being the most rigorous and general framework for quantum transport, the non-equilibrium Green's function method has two weaknesses. First of all, it is difficult to develop approximations that maintain charge and current conservation. Secondly, numerical solutions of the NEGF equations for realistic quantum devices are extremely demanding and time consuming.

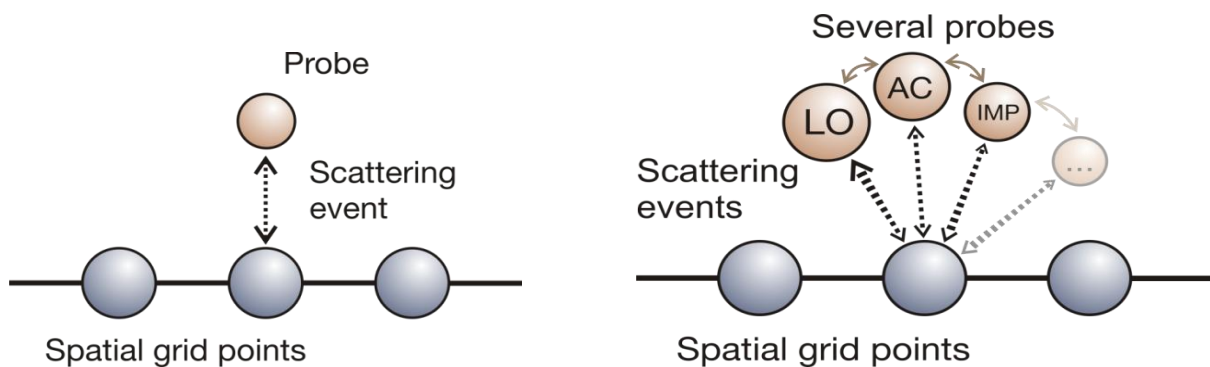


Figure 3: Left: The standard Buttiker probe model associates a single momentum and energy sink with each device node in position space. Right: The present multi-scattering Buttiker probe model accounts for individual scattering mechanisms by using multiple probes for each node

We have developed a novel method (Greck 2010) that we termed multi-scattering Buttiker probe model (MSB). It generalizes the standard Buttiker model approach (Büttiker 1986, Venugopal 2003) by taking into account individual scatterings mechanisms, as illustrated in Fig. 3, ensures exact current conservation, and is orders of magnitude faster than the full NEGF method.

The key simplifications (Greck 2010) consist in two steps. First, we side-step the self-consistent solutions of G^R and $G^<$. This is achieved by approximating the lesser Green's function by its form for an equilibrium system, albeit with a local Fermi level. The latter is determined in such a way as to guarantee current conservation.

The second step consists in performing the momentum-integration analytically so that the Green's functions become functions of space and energy only. The self-energy includes scattering by acoustic and optical phonons, impurity scattering and the coupling to the contacts. These various self-energies are adjusted to bulk scattering rates and depend on the material, temperature and carrier density.

As an application, we consider the current-voltage characteristics of a GaAs/AlGaAs THz quantum cascade structure consisting of 4 quantum wells per period in the active region. In

Fig. 4, we compare the results of fully self-consistent NEGF calculations for two different carrier concentrations with results obtained by the present MSB model. As one can see, one obtains very satisfactory agreement. The computer time required for the full NEGF calculation of the I-V characteristics amounts to roughly 1 week, whereas the MSB model took less than 1 hour.

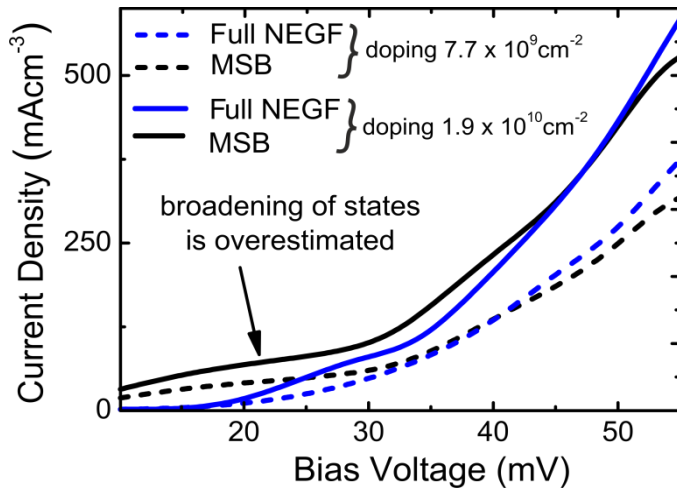


Figure 4: I-V characteristics of a GaAs/AlGaAs THz quantum cascade structure for two different doping densities

Mesoscopic electronic structure theory of antimonide compounds

The recent fabrication of high quality and high mobility antimonide heterostructures has revived the interest in this material class since their widely tunable electronic structure and optical properties offer many possibilities to enhance the gain for intersubband or even interband based laser structures in the mid-infrared by band structure engineering (Dente 1999, Semenikhin 2007, Liu 2002). In combination with arsenide materials, antimonides can form type-II heterostructures with a broken gap which makes them particularly promising candidates for infrared lasers. Unfortunately, mesoscopic quantum well systems with broken gaps are difficult to deal with in terms of standard theoretical band structure techniques such as effective mass theory. Once there is no gap, the chemical potential must be determined explicitly. However, standard effective mass theory tacitly assumes that electron and hole states are well separated from each other so that they can be occupied independently. Consequently, only few theoretical approaches have been developed so far to predict the electronic structure of nanostructures with broken gaps (Liu 2002, Altarelli 1983, Xu 2007). Within this project, we have developed a novel electronic structure scheme for broken-gap materials that maintains the efficiency of a continuum approach that yet does not depend on a separation into negatively charged electron and positively charged hole states.

We have developed a novel charge self-consistent eight-band k^*p envelope function method for the calculation of the electronic structure of type-II broken-gap heterostructures. Standard multiband k^*p approaches fail to yield the correct occupation of electronic states in broken-gap heterostructures, because the strong hybridization of conduction band and valence band

states is incompatible with the separate occupation of electron and hole states that is common to envelope function approaches. In our method, we occupy all included subbands with electrons according to the Fermi statistics and subsequently subtract a positive background ionic charge that guarantees charge neutrality. With this procedure, we have calculated local charge densities and subband dispersions of periodically n and p doped layers of GaAs as well as effective band gaps of intrinsic InAs/GaSb superlattices.

Here, we consider intrinsic InAs/GaSb (001)-superlattices that have been fabricated and studied experimentally (Poulter 1999, Wei 2004). The structures are characterized by the InAs and GaSb layer widths w_1 and w_2 , respectively. In Fig. 5, we schematically depict the bulk band edges of the conduction band E_C (dotted line) and the heavy hole valence band E_V (solid line) for two different regimes of layer widths. The graphs show a type-II broken-gap band alignment with an overlap between E_C in the InAs layer and E_V in the GaSb layer.

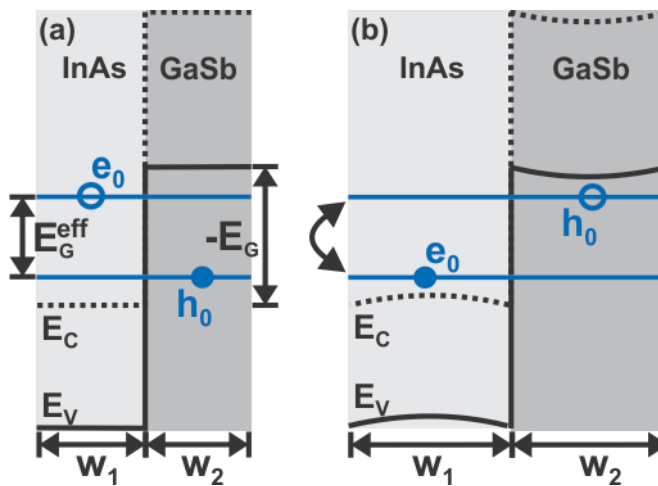


Figure 5: Schematic band structure of InAs/GaSb superlattice with InAs and GaSb layer widths w_1 and w_2 , respectively. (a) Sketch of the broken bulk band edges (dashed: conduction bands, full: heavy hole bands) for narrow layer widths with negative gap in position space. The lowest unoccupied (labeled by e_0) and highest occupied (labeled by h_0) superlattice subbands are also shown and lead to a positive effective band gap (b) Same as in (a) for larger layer widths. The character of the lowest unoccupied and highest occupied subbands is reversed. The effective band gap is still positive but there is a charge transfer between the adjacent layers that leads to a band bending as indicated schematically

Confinement leads to subbands that are derived from the bulk InAs conduction band and lie above E_C , as well as to subbands that are derived from the bulk GaSb heavy hole band and lie below E_V . In Fig. 5, we show the lowest of the former states (e_0) and the highest of the latter states (h_0). For small layer widths (typically $w_1, w_2 < 9$ nm), the energy difference $E(e_0) - E(h_0)$ is positive, leading to a conventional semiconductor. This situation is shown in Fig. 5(a). For larger layer widths (Fig. 5(b)), the ordering of InAs and GaSb bulk derived subbands gets switched due to the weaker confinement. In such situations, a self-consistent calculation of the Fermi level and consideration of the entire subbands is required to determine the effective band gap. As indicated schematically in Fig. 5(b), the mixing of occupied InAs- and GaSb-like states causes a significant amount of charge transfer that leads to band bending.

We now vary the InAs layer widths w_1 from 4 to 30 nm and assume a fixed GaSb layer width of $w_2 = 10$ nm for a temperature of $T = 4$ K. The results are summarized in Fig. 6. For the

smallest layer widths, strong confinement raises the lowest unoccupied subband above the highest occupied subband leading to a positive effective band gap in accordance with Fig. 5(a). With increasing layer width w_1 , the reduced confinement leads to a decrease in the effective band gap. At $w_1 < 9$ nm, the effective band gap becomes zero. By further increasing w_1 , the subbands e_0 and h_0 swap their energetic positions and an anticrossing gap opens. The effective band gap remains positive, but the highest occupied (HO) and lowest unoccupied (LU) states have changed. Thus, the effective gap now increases as a consequence of the reduction in confinement. When the InAs layer width is further increased to $w_1 > 10$ nm, we find the extrema of the LU and HO subbands to be located at different values of the in-plane wave vector. Thus, the superlattice becomes an indirect gap semiconductor. By further increasing w_1 , the effective gap decreases and even becomes negative for $w_1 > 21$ nm. Thus, our results confirm the existence of a semiconductor-semimetal transition that has been predicted before (Magri 2000).

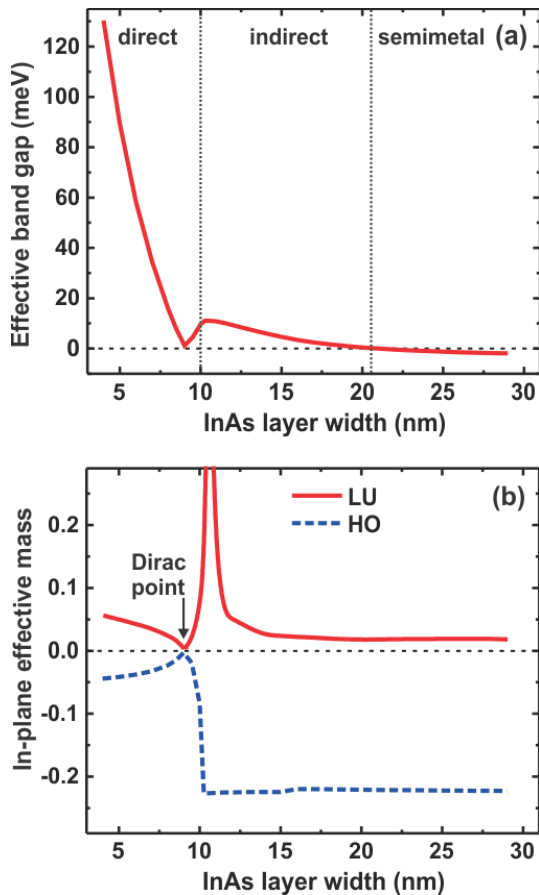


Figure 6: (a) Calculated effective band gap of InAs/GaSb superlattices as a function of the InAs layer width for a fixed GaSb layer width of 10 nm. The vertical dotted lines indicate regimes where the band structure corresponds to a direct semiconductor, an indirect semiconductor, and a semimetal, respectively. (b) Calculated in-plane effective masses of lowest unoccupied (LU) and highest occupied (HO) subband extrema for the same structure. The Dirac point indicates a situation where the in-plane subband dispersion becomes linear

In Fig. 6(b), we show the calculated LU and HO in-plane effective masses along the [110] direction. Starting from the smallest layer widths, both LU and HO effective masses decrease in magnitude with increasing InAs layer width. Interestingly, they become zero when the effective band gap vanishes ($w_1 \sim 9$ nm). At this point, our results indicate that the electrons in the InAs/GaSb superlattice layers become a two-dimensional gas of mass-less Dirac fermions, similar to the situation known from graphene.

4.13.4 Collaboration within and beyond the SFB

We have been and still are intensely collaborating with the experimental groups in Vienna within this SFB who design, measure, and grow novel THz QCL structures as well as with the experimental groups in Linz who investigate the optical properties of various SiGe quantum dot structures. In addition, we are collaborating with many other experimental and theory groups in Austria (Graz), France (Paris), Germany (Munich, Regensburg), Japan (Tokyo, Tsukuba), and USA (Buffalo, Purdue). Up to now, 3 papers have been published together with the IR-ON experimental groups (Deutsch 2010, Kubis 2009d, Brehm 2008), but we anticipate several more to come since many of our improved QCL designs have yet to be tested experimentally.

Our main current collaboration consists in the design of the embedded or core-shell type quantum wire based QCL structures since they promise room temperature lasing.

Our QCL calculations have revealed that a large portion of the current through THz QCLs is maintained by coherent multibarrier tunnelling which leads to electron distributions that do not follow the periodicity of the QCL which in turn diminishes the overall gain. We have proposed several alternative designs consisting of either less or more quantum wells that should yield a significantly higher gain (Kubis 2008, Kubis 2009/a-c). These experiments are currently being prepared and performed.

In a collaboration with Prof. Hirakawa from Tokyo university (Yasuda 2009), we have predicted a novel four-level scheme terahertz QCL where the upper laser state gets populated by LO phonons rather than by resonant tunnelling. This leads to a significantly higher gain than conventional designs, albeit only for temperatures less than 200 K.

We have performed NEGF as well as empirical electronic structure calculations of terahertz quantum cascade lasers based on the $\text{In}_{.53}\text{Ga}_{.47}\text{As}/\text{GaAs}_{.51}\text{Sb}_{.49}$ type II material system that the Vienna group succeeded to fabricate. In fact, the theory group of Bechstedt and Kresse provided highly accurate ab initio electronic structure calculations which provided another essential ingredient in this collaboration.

4.13.5 References

- Altarelli M. (1983), Electronic structure and semiconductor-semimetal transition in InAs-GaSb superlattices, Phys. Rev. B 28, 842-845, [DOI: 10.1103/PhysRevB.28.842](https://doi.org/10.1103/PhysRevB.28.842)
- Brehm M., T. Suzuki, Z. Zhong, T. Fromherz, J. Stangl, G. Hesser, S. Birner, F. Schäffler, G. Bauer (2008), Bandstructure and photoluminescence of SiGe islands with controlled Ge concentration, Microelectronics Journal 39, 485, [DOI: 10.1016/j.mejo.2007.07.111](https://doi.org/10.1016/j.mejo.2007.07.111)
- Büttiker M. (1986), Four-Terminal Phase-Coherent Conductance, Phys. Rev. Lett. 57, 1761-1764, [DOI: 10.1103/PhysRevLett.57.1761](https://doi.org/10.1103/PhysRevLett.57.1761)
- Dente G. C. and M. L. Tilton (1999), Pseudopotential methods for superlattices: Applications to mid-infrared semiconductor lasers, J. Appl. Phys. 86, 1420-1429, [DOI: 10.1063/1.370905](https://doi.org/10.1063/1.370905)
- Deutsch C., A. Benz, H. Detz, P. Klang, M. Nobile, A. M. Andrews, W. Schrenk, T. Kubis, P. Vogl, G. Strasser and K. Unterrainer (2010), Terahertz Quantum Cascade Lasers based on Type II InGaAs/GaAsSb/InP, App. Phys. Lett. 97, 261110, [DOI: 10.1063/1.3532106](https://doi.org/10.1063/1.3532106)
- Dmitriev I. A. and R. A. Suris (2005), Quantum cascade lasers based on quantum dot superlattice, phys. stat. sol. (a) 202, No. 6, 987-991, [DOI: 10.1002/pssa.200460714](https://doi.org/10.1002/pssa.200460714)
- Grange T., R. Ferreira and G. Bastard (2007), Polaron relaxation in self-assembled quantum dots: Breakdown of the semiclassical model, Phys. Rev. B 76, 241304(R), [DOI: 10.1103/PhysRevB.76.241304](https://doi.org/10.1103/PhysRevB.76.241304)
- Greck P., C. Schindler, T. Kubis and P. Vogl (2010), The nonequilibrium Green's functions method and descendants: ways to avoid and to go, IWCE Conference Proceedings 2010, [DOI: 10.1109/IWCE.2010.5677996](https://doi.org/10.1109/IWCE.2010.5677996)
- Jirauschek C., G. Scarpa, P. Lugli, M.S. Vitiello and G. Scamarcio (2007), Comparative analysis of resonant phonon THz quantum cascade lasers, Journal of Applied Physics 101 (8) 086109, [DOI: 10.1063/1.2719683](https://doi.org/10.1063/1.2719683)
- Kubis T. and P. Vogl (2011), Assessment of approximations in nonequilibrium Green's function theory, Phys. Rev. B 83, 195304, [DOI: 10.1103/PhysRevB.83.195304](https://doi.org/10.1103/PhysRevB.83.195304)
- Kubis T. and P. Vogl (2009a), How periodic are terahertz quantum cascade lasers?, Journal of Physics: Conference Series 193, 012063, [DOI: 10.1088/1742-6596/193/1/012063](https://doi.org/10.1088/1742-6596/193/1/012063)
- Kubis T. and P. Vogl (2009b), Predictive quantum theory of current and optical emission in quantum cascade lasers, Proc. SPIE 7230, 723019, [DOI: 10.1117/12.808483](https://doi.org/10.1117/12.808483)
- Kubis T. and P. Vogl (2009c), Predictive Quantum Theory of Current and Optical Gain in Quantum Cascade Lasers, Laser Physics 19, 762, [DOI: 10.1134/S1054660X0904032X](https://doi.org/10.1134/S1054660X0904032X)
- Kubis T., C. Yeh, P. Vogl, A. Benz, G. Fasching and C. Deutsch (2009d), Theory of nonequilibrium quantum transport and energy dissipation in terahertz quantum cascade lasers, Phys. Rev. B 79, 195323, [DOI: 10.1103/PhysRevB.79.195323](https://doi.org/10.1103/PhysRevB.79.195323)
- Kubis T., C. Yeh and P. Vogl (2008), Non-equilibrium quantum transport theory: current and gain in quantum cascade lasers, Journal of Computational Electronics Vol. 7, 432-435, [DOI: 10.1007/s10825-007-0158-2](https://doi.org/10.1007/s10825-007-0158-2)

- Lake R., G. Klimeck, R.C. Bowen and D. Jovanovic (1997), Single and multiband modeling of quantum electron transport through layered semiconductor devices, *J. Appl. Phys.* 81, 7845, [DOI: 10.1063/1.365394](https://doi.org/10.1063/1.365394)
- Lee S.-C. and A. Wacker (2002), Nonequilibrium Green's function theory for transport and gain properties of quantum cascade structures, *Phys. Rev. B* 66, 245314, [DOI: 10.1103/PhysRevB.66.245314](https://doi.org/10.1103/PhysRevB.66.245314)
- Liu G. and S.-L. Chuang (2002), Modeling of Sb-based type-II quantum cascade lasers, *Phys. Rev. B* 65, 165220, [DOI: 10.1103/PhysRevB.65.165220](https://doi.org/10.1103/PhysRevB.65.165220)
- Magri R., L. W. Wang, A. Zunger, I. Vurgaftman and J. R. Meyer (2000), Anticrossing semiconducting band gap in nominally semimetallic InAs/GaSb superlattices, *Phys. Rev. B* 61, 10235, [DOI: 10.1103/PhysRevB.61.10235](https://doi.org/10.1103/PhysRevB.61.10235)
- Poulter A. J. L., M. Lakrimi, R. J. Nicholas, N. J. Mason and P. J. Walker (1999), Intersubband transitions in InAs/GaSb semimetallic superlattices, *Phys. Rev. B* 59, 10785, [DOI: 10.1103/PhysRevB.59.10785](https://doi.org/10.1103/PhysRevB.59.10785)
- Savic I., N. Vukmirovic, Z. Ikonc, D. Indjin, R. W. Kelsall, P. Harrison and V. Milanovic (2007), Density matrix theory of transport and gain in quantum cascade lasers in a magnetic field, *Phys. Rev. B* 76, 165310, [DOI: 10.1103/PhysRevB.76.165310](https://doi.org/10.1103/PhysRevB.76.165310)
- Schmielau T. and M. F. Pereira (2009), Impact of momentum dependent matrix elements on scattering effects in quantum cascade lasers, *phys. stat. sol. (b)* 246, 329, [DOI: 10.1002/pssb.200880328](https://doi.org/10.1002/pssb.200880328)
- Semenikhin I., A. Zakharova, K. Nilsson and K. A. Chao (2007), Effects of bulk inversion asymmetry and low interface symmetry on the optical properties of broken-gap heterostructures, *Phys. Rev. B* 76, 035335, [DOI: 10.1103/PhysRevB.76.035335](https://doi.org/10.1103/PhysRevB.76.035335)
- Venugopal R., M. Paulsson, S. Goasguen, S. Datta and M. Lundstrom (2003), A simple quantum mechanical treatment of scattering in nanoscale transistors, *J. Appl. Phys.* 93, 5613, [DOI: 10.1063/1.1563298](https://doi.org/10.1063/1.1563298)
- Vogl P. and T. Kubis (2010), The non-equilibrium Green's function method: an introduction, *Journal of Computational Electronics* 9, 3-4, 237-242, [DOI: 10.1007/s10825-010-0313-z](https://doi.org/10.1007/s10825-010-0313-z)
- Vukmirovic N., Z. Ikonc, D. Indjin and P. Harrison (2008), Electron Transport and Terahertz Gain in Quantum-Dot Cascades, *IEEE Photonics Techn. Lett.* 20, 129, [DOI: 10.1109/LPT.2007.912533](https://doi.org/10.1109/LPT.2007.912533)
- Vukmirovic N., Z. Ikonc, D. Indjin and P. Harrison (2007), Quantum transport in semiconductor quantum dot superlattices: Electron-phonon resonances and polaron effects, *Phys. Rev. B* 76, 245313, [DOI: 10.1103/PhysRevB.76.245313](https://doi.org/10.1103/PhysRevB.76.245313)
- Wacker A. (2002), Semiconductor superlattices: a model system for nonlinear transport, *Phys. Rep.* 357, 1, [DOI: 10.1016/S0370-1573\(01\)00029-1](https://doi.org/10.1016/S0370-1573(01)00029-1)
- Wei Y. and M. Razeghi (2004), Modeling of type-II InAs/GaSb superlattices using an empirical tight-binding method and interface engineering, *Phys. Rev. B* 69, 085316, [DOI: 10.1103/PhysRevB.69.085316](https://doi.org/10.1103/PhysRevB.69.085316)
- Wingreen N. S. and C. A. Stafford (1997), Quantum-Dot Cascade Laser: Proposal for an Ultralow-Threshold Semiconductor Laser, *IEEE J. Quantum Electronics* 33, 1170, [DOI: 10.1109/3.594880](https://doi.org/10.1109/3.594880)
- Xu W., X. F. Wei and J. Zhang (2008), Exchange-induced terahertz minigap in InAs/GaSb type II and broken-gap quantum wells, *Appl. Phys. Lett.* 92, 162108, [DOI: 10.1063/1.2913757](https://doi.org/10.1063/1.2913757)

Xu W., P. A. Folkes and G. Gumbs (2007), Self-consistent electronic subband structure of undoped InAs/GaSb-based type II and broken-gap quantum well systems, J. Appl. Phys. 102, 033703, [DOI: 10.1063/1.2759873](https://doi.org/10.1063/1.2759873)

Yasuda H., T. Kubis, P. Vogl, N. Sekine, I. Hosako and K. Hirakawa (2009), Nonequilibrium Green's function calculation for four-level scheme terahertz quantum cascade lasers, Appl. Phys. Lett. 94, 151109, [DOI: 10.1063/1.3119312](https://doi.org/10.1063/1.3119312)

Zibik E. A., T. Grange, B. A. Carpenter, N. E. Porter, R. Ferreira, G. Bastard, D. Stehr, S. Winnerl, M. Helm, H. Y. Liu, M. S. Skolnick and L. R. Wilson (2009), Long lifetimes of quantum-dot intersublevel transitions in the terahertz range, Nature Materials 8, 803-807, [DOI: 10.1038/nmat2511](https://doi.org/10.1038/nmat2511)

For a complete list of publications of this project part please refer to p. 66 (2.1 List of publications)!